LGN regulates mitotic spindle orientation during epithelial morphogenesis

Zhen Zheng,[1,4] Huabin Zhu,[1] Qingwen Wan,[1] Jing Liu,[1,5] Zhuoni Xiao,[1] David P. Siderovski,[3] and Quansheng Du[1,2]

[1]Institute of Molecular Medicine and Genetics and [2]Department of Neurology, Medical College of Georgia, Augusta, GA 30912
[3]Department of Pharmacology, University of North Carolina at Chapel Hill, Chapel Hill, NC 27599
[4]Division of Nephrology, Renmin Hospital, and [5]School of Pharmacy, Wuhan University, Wuhan 430072, China

Coordinated cell polarization and mitotic spindle orientation are thought to be important for epithelial morphogenesis. Whether spindle orientation is indeed linked to epithelial morphogenesis and how it is controlled at the molecular level is still unknown. Here, we show that the NuMA- and Gα-binding protein LGN is required for directing spindle orientation during cystogenesis of MDCK cells. LGN localizes to the lateral cell cortex, and is excluded from the apical cell cortex of dividing cells. Depleting LGN, preventing its cortical localization, or disrupting its interaction with endogenous NuMA or Gα proteins all lead to spindle misorientation and abnormal cystogenesis. Moreover, artificial mistargeting of endogenous LGN to the apical membrane results in a near 90° rotation of the spindle axis and profound cystogenesis defects that are dependent on cell division. The normal apical exclusion of LGN during mitosis appears to be mediated by atypical PKC. Thus, cell polarization–mediated spatial restriction of spindle orientation determinants is critical for epithelial morphogenesis.

Introduction

The position of the mitotic spindle determines the cleavage plane of the mother cell (Rappaport, 1971). The activity of cortical cues, either intrinsic or extrinsic, may determine spindle orientation through regulation of the interaction between astral microtubules (MTs) and the cell cortex (Ahringer, 2003; Colombo et al., 2003; Grill et al., 2003; Grill and Hyman, 2005; Siegrist and Doe, 2006; Théry and Bornens, 2006; Théry et al., 2007). Studies of a specific type of cell division—asymmetric cell division in the *Caenorhabditis elegans* zygote and *Drosophila* neuroblast—have shed light on the molecular mechanisms of mitotic spindle orientation (Betschinger and Knoblich, 2004; Roegiers and Jan, 2004; Siller and Doe, 2009). Cell polarization leads to asymmetric cortical distribution of an evolutionarily conserved protein complex: Mud–Pins–Gα in *Drosophila* and Lin5–GPR1,2–Gα in *C. elegans*, which directs spindle orientation and subsequent asymmetric cell division (Bowman et al., 2006; Izumi et al., 2006; Siller et al., 2006; Couwenbergs et al., 2007; Park and Rose, 2008). The mammalian counterpart of this protein complex, NuMA/LGN/Gα, is also capable of generating pulling forces on astral MTs during mitosis (Du and Macara, 2004). In fact, LGN functions as a conformational switch that links Gα and NuMA (Du and Macara, 2004; Tall and Gilman, 2005). Recently, it has been shown that LGN is required for proper spindle orientation in neuronal progenitor cells during neurogenesis in mice and chicken (Morin et al., 2007; Konno et al., 2008). Whether the NuMA–LGN–Gα protein complex also regulates spindle orientation in other cells is unknown.

Epithelial morphogenesis involves the sensing of extracellular cues by individual cells and the interaction between neighboring cells (Bryant and Mostov, 2008). Coordination between cell polarization (e.g., specification of apical and basal membrane, formation of adherens junctions and tight junctions), cytoskeleton reorganization, and directional vesicle trafficking contributes to the establishment of polarized tissue. During morphogenesis, epithelial cells usually divide symmetrically to generate two identical daughter cells. The correct orientation of cell division has been proposed to be important for the integrity of epithelial sheets as well as tissue elongation and

Correspondence to Quansheng Du: qdu@mcg.edu

Abbreviations used in this paper: aPKC, atypical protein kinase C; Crb3, Crumbs3; Gα, the alpha subunit of the heterotrimeric G proteins; Gαi, the alpha subunit of adenylyl cyclase–inhibitory heterotrimeric G proteins; GoLoco motif, $G\alpha_{i/o}$-Loco motif; LGN, mammalian homologue of Pins; MT, microtubule; NuMA, nuclear mitotic apparatus protein; Pins, partner of inscuteable.

The Rockefeller University Press $30.00
J. Cell Biol. Vol. 189 No. 2 275–288
www.jcb.org/cgi/doi/10.1083/jcb.200910021

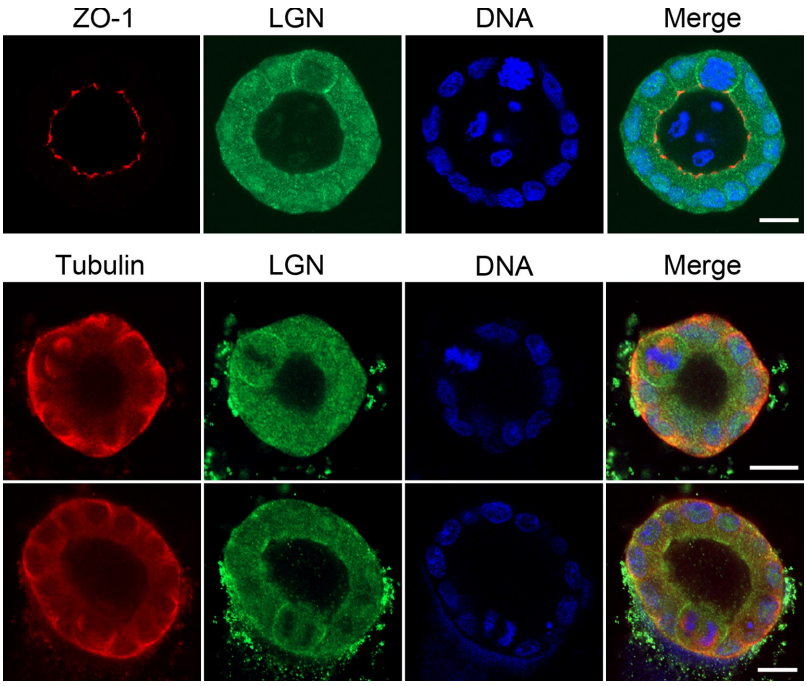

Figure 1. **LGN is enriched at the lateral cortex of mitotic MDCK cells during cystogenesis.** MDCK II cells were plated in matrigel for 4 d to allow cystogenesis. Cysts were fixed and immunostained for LGN (green), ZO-1 (red), and α-tubulin (red). DNA was stained with Hoechst 33342 (blue). Single confocal sections through the middle region of the cysts are shown. Bar, 20 µm.

shaping (Baena-López et al., 2005; Saburi et al., 2008; Segalen and Bellaïche, 2009). Recently, in a 3D Caco-2 cell system, Jaffe et al. (2008) showed that the cystogenesis defect in Cdc42 knockdown cells correlated with altered spindle orientation. However, a definite link between spindle orientation and epithelial morphogenesis is still missing. Moreover, the molecular identity of the cortical cues that direct spindle orientation in symmetrically dividing mammalian cells during morphogenesis is still elusive.

Here, we present a molecular mechanism critical for appropriate spindle orientation during epithelial morphogenesis in a 3D Madin Darby canine kidney (MDCK) cell-based system. We show that LGN is spatially restricted to the lateral cell cortex in dividing MDCK cells during cystogenesis and functions with its binding partners, NuMA and Gα, to direct spindle orientation. Our results indicate that properly oriented cell division is required for normal epithelial morphogenesis.

Results

LGN localizes at the lateral cell cortex in mitotic cells during cystogenesis of MDCK cells cultured in matrigel

LGN is known to be a mitosis-specific cortical protein in 2D cultured monolayers of different cell types (Kaushik et al., 2003; Du and Macara, 2004). To assess the distribution of LGN during cystogenesis, we stained MDCK cysts grown in matrigel using anti-LGN antibodies. Consistent with 2D cultured cells, cortical LGN staining was seen only in mitotic cells from prophase until the end of telophase (Fig. 1). Interestingly, LGN localized predominantly at the lateral cell cortex and appeared to be absent from the apical cell cortex, as revealed by costaining of the tight junction protein ZO-1, which localizes to the apical sites of the cell–cell contact (Fig. 1, top). We also co-stained the cysts with anti–α-tubulin antibody to reveal the mitotic spindle. In agreement with a previous analysis of mitotic spindles of MDCK cysts grown in collagen gels (Yu et al., 2003) and a more recent study of Caco-2 cells (Jaffe et al., 2008), the spindle poles, and presumably the astral MTs were always facing the lateral cell cortex from metaphase onwards (Fig. 1, bottom panels), suggesting that mechanisms exist to control spindle orientation during cystogenesis. The correlation between LGN localization and spindle orientation, and the fact that LGN is capable of specifying force generation on astral MTs (Du and Macara, 2004) prompted us to further study the function of LGN during cystogenesis.

Reduction of LGN expression levels results in spindle misorientation and defective cystogenesis

Lentivirus-mediated expression of short hairpin RNA (shRNA) was applied to knockdown LGN expression in a stable fashion in MDCK cells. Stably transduced cell lines were isolated based on virus-mediated expression of GFP. LGN expression was efficiently knocked down by two different lentiviruses (LGN-KD1 and LGN-KD2) expressing shRNAs targeting different sequences of canine LGN (Fig. 2 A). The cortical staining of LGN in mitotic cells was also dramatically reduced in LGN knockdown cells (Fig. 2 B). Unlike previously observed effect in HeLa and HEK293 cells (Du et al., 2001; Yasumi et al., 2005), knockdown of LGN in MDCK cells did not cause obvious mitotic defects, as judged by the morphology of mitotic spindles and cell proliferation analysis (Fig. S1).

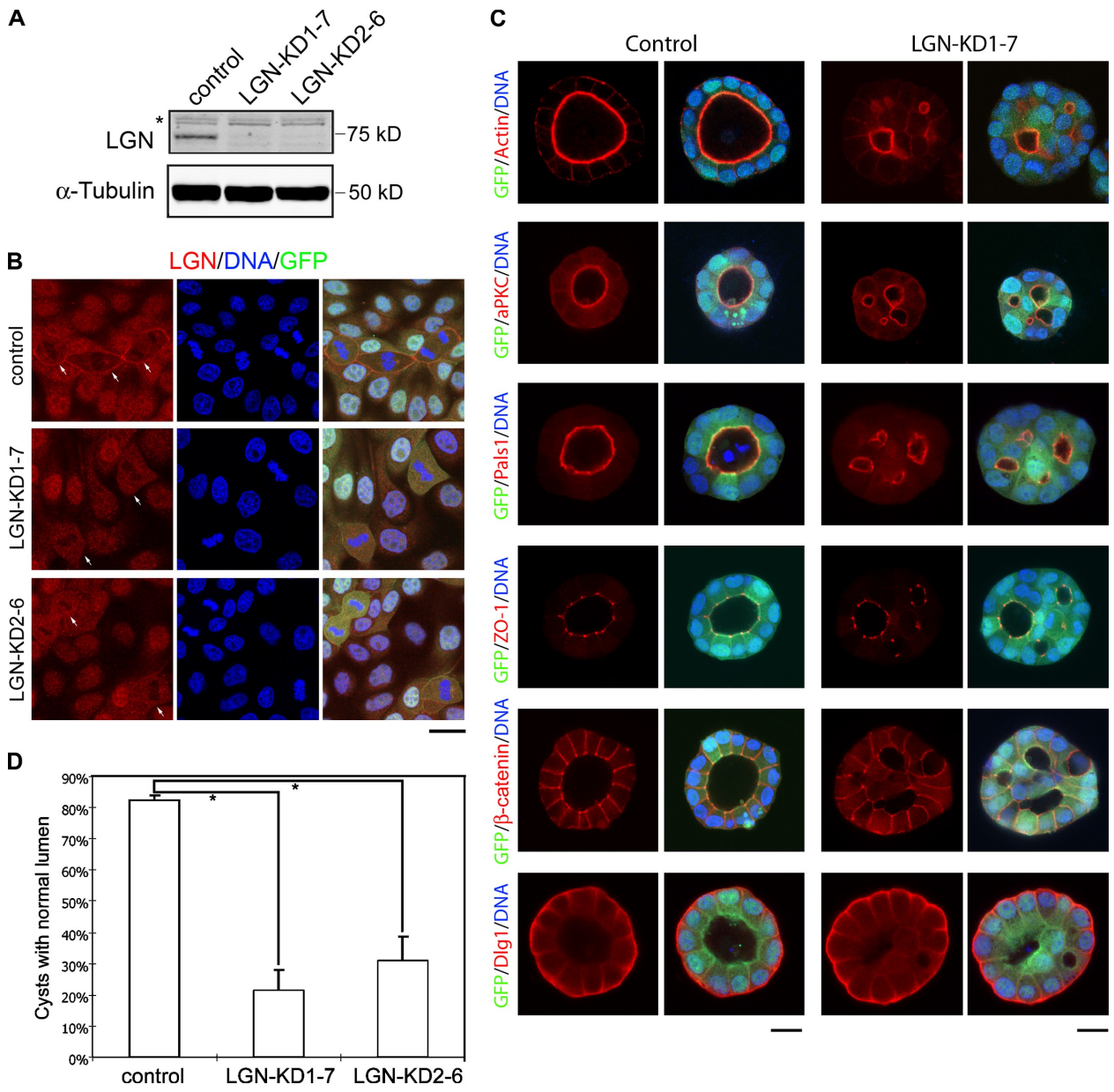

Figure 2. **Knockdown of LGN in MDCK cells results in defective cystogenesis.** (A) Western blot analysis of representative cell lines stably transduced by control or two different lentiviruses expressing shRNAs against LGN (LGN-KD1-7 and LGN-KD2-6). Total cell lysates were blotted for LGN and α-tubulin. The asterisk indicates nonspecific bands. (B) The cortical staining of LGN in mitotic cells is significantly reduced in LGN knockdown cells. Control, LGN-KD1-7, and LGN-KD2-6 MDCK cells were fixed and immunostained for LGN (red). DNA was stained with Hoechst 33342 (blue). The merged images are also shown (right). Note that these lentivirus-transduced cell lines express GFP. Arrows point to mitotic cells. (C) Knockdown of LGN induces multiple lumens but does not affect cell polarization. Control (left panels) or LGN KD1-7 (right panels) cells were plated in matrigel for 3–4 d. Cysts were fixed and immunostained to detect aPKC, Pals1, ZO-1, β-catenin, and Dlg1 (red). Actin was stained with rhodamine phalloidin (red, top). Single confocal sections through the middle region of the cysts are shown. Bars, 20 μm. (D) Quantitation of cysts with single normal lumen in control, LGN KD1-7, or LGN KD2-6 cells. Values are mean ± SD from three independent experiments; $n > 100$ cysts/experiment. *, $P < 0.01$.

Transduced cells were then plated in matrigel for cystogenesis. As previously reported (O'Brien et al., 2002; Martin-Belmonte et al., 2007), the majority of control virus–transduced MDCK cells formed spherical cysts consisting of single-layered cells surrounding a central lumen that is mostly free of cells (Fig. 2 C). In contrast, cysts formed from LGN knockdown cells, although growing to similar size as cysts from control cells, frequently showed accumulation of cells in the center of the cysts, suggesting abnormal cystogenesis (Fig. 2 C). During cystogenesis, F-actin is enriched at the apical membrane facing the central lumen and is generally used as a marker to monitor lumen formation. As revealed by F-actin staining, more than 80% of control cysts (82.5 ± 1.4%) showed single lumen formation (Fig. 2 C, top; Fig. 2 D). However, only 20–30% of LGN knockdown cysts formed a single lumen while the rest frequently developed multiple, F-actin–delimited, small lumens (Fig. 2 C, top; Fig. 2 D, 21.5 ± 6.6% of LGN-KD1-7 and 30.9 ± 7.8% of LGN-KD2-6 cysts formed single lumen; Fig. S2 B). The abnormal lumen formation was observed in multiple independent cell lines transduced by LGN-KD1

or LGN-KD2 lentiviruses (Fig. 2, C and D; Fig. S2 B and unpublished data), suggesting that the defect is caused by reduced expression of LGN.

The multi-luminal phenotype could be attributed to cell polarity defects and subsequent malformation of the apical membrane (Martin-Belmonte et al., 2007; Horikoshi et al., 2009). We thus carefully compared the localization of multiple polarity proteins in control and LGN knockdown cysts. As shown in Fig. 2 C and Fig. S2 B, aPKC (atypical PKC) and Pals1 (protein associated with Lin seven-1) were still enriched at the apical membrane of the multiple small lumens in LGN knockdown cysts. The tight junction marker ZO-1 was restricted to the apical cell–cell contact region. The basal lateral proteins, β-catenin and Dlg1 (Discs large-1), were excluded from the apical membrane in both control and LGN knockdown cysts. Thus, the overall cell polarization appears to be normal in LGN knockdown cysts.

The potential link between LGN and spindle orientation prompted us to check whether spindle orientation was affected in LGN knockdown cysts. We examined mitotic spindles in cysts by anti-tubulin antibody staining. In control cysts, the spindles were predominantly perpendicular to the apical–basal axis (Fig. 3 A, top). However, in LGN knockdown cysts, the position of mitotic spindles was frequently observed to be tilted or parallel to the apical–basal axis (Fig. 3 A, bottom two panels). In contrast to this altered positioning, the morphology of mitotic spindles in LGN knockdown cysts was indistinguishable from that of the control cysts, suggesting that the spindle organization was normal. We then quantified metaphase spindle orientation by measuring the angle of each spindle axis in relation to the center of the apical membrane, as depicted in Fig. 3 B. Consistent with our observation, in control cysts the orientation of the spindle was predominantly orthogonal to the apical–basal axis (mean angle = 77.5 ± 2.0°). However, in LGN knockdown cysts the spindle orientation was almost randomized (mean angle = 43.6 ± 3.8° for LGN-KD1-7 cysts; mean angle = 47.4 ± 4.4° for LGN-KD2-6 cysts). Consistent with a previous report that spindle orientation was predominantly set at metaphase during cystogenesis of MDCK cells (Yu et al., 2003), quantitation of anaphase spindle orientation gave a similar result as that of metaphase spindles (Fig. S2 A). Importantly, the distribution of polarity proteins in mitotic LGN knockdown cells was not obviously altered as compared with that of control cells (Fig. S2 B). Taken together, without an obvious effect on cell polarization, depletion of LGN expression in MDCK cells results in spindle misorientation and defective cystogenesis.

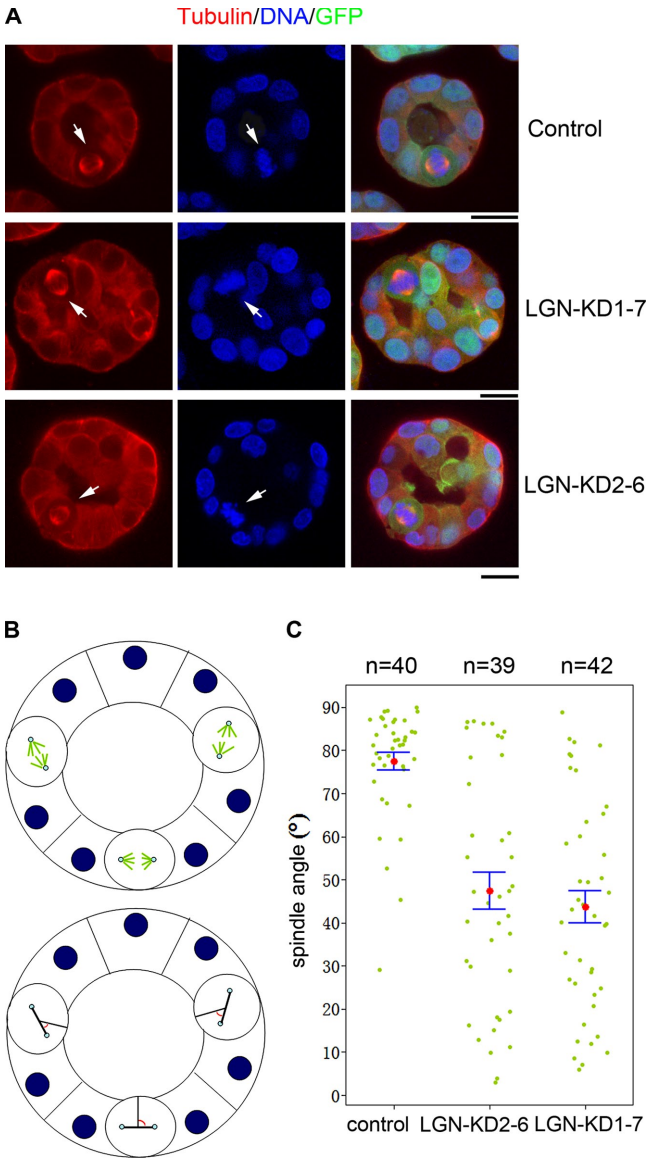

Figure 3. **LGN depletion disrupts mitotic spindle orientation during cystogenesis.** (A) Control, LGN-KD1-7, and LGN-KD2-6 MDCK cells were cultured in matrigel for 3–4 d. Cysts were fixed and immunostained for α-tubulin (red). DNA was stained with Hoechst 33342 (blue). Single confocal sections through the middle region of the cysts are shown. Arrows indicate mitotic cells. Bars, 20 µm. (B) Diagram depicting spindle angle measurement. Cysts grown for 3–4 d were fixed and stained with anti–α-tubulin antibody (green) and Hoechst 33342 (blue). Confocal images of metaphase cells in the middle region of the cysts were collected. A line was drawn to connect the two spindle poles (thick black lines). Another line was drawn from the centroid of the apical domain to the midpoint of the spindle axis (thin black lines), and the acute angle (red) between the two lines was analyzed. (C) Scatter diagram of metaphase spindle angles in control, LGN-KD1-7, and LGN-KD2-6 cysts. Results were from three independent experiments. Pink dots indicate mean values, green dots indicate individual data points, and error bars represent the SEM of the total number of spindles analyzed.

Preventing the cortical localization of LGN also leads to spindle misorientation and defective cystogenesis

The C terminus of LGN contains four GoLoco repeats that specifically bind to the α subunit of adenylyl cyclase–inhibitory heterotrimeric G proteins (Gαi) in its GDP-bound state (Bernard et al., 2001; Willard et al., 2004; McCudden et al., 2005). We showed previously that overexpression of a nonmembrane-bound form of Gαi results in sequestration of LGN in the cytosol in mitotic cells (Du and Macara, 2004). We reasoned that, if cortical LGN is required for directing spindle orientation during cystogenesis, then preventing the cortical localization of LGN will affect LGN function and lead to a similar phenotype as LGN knockdown. To test this hypothesis, we generated stable

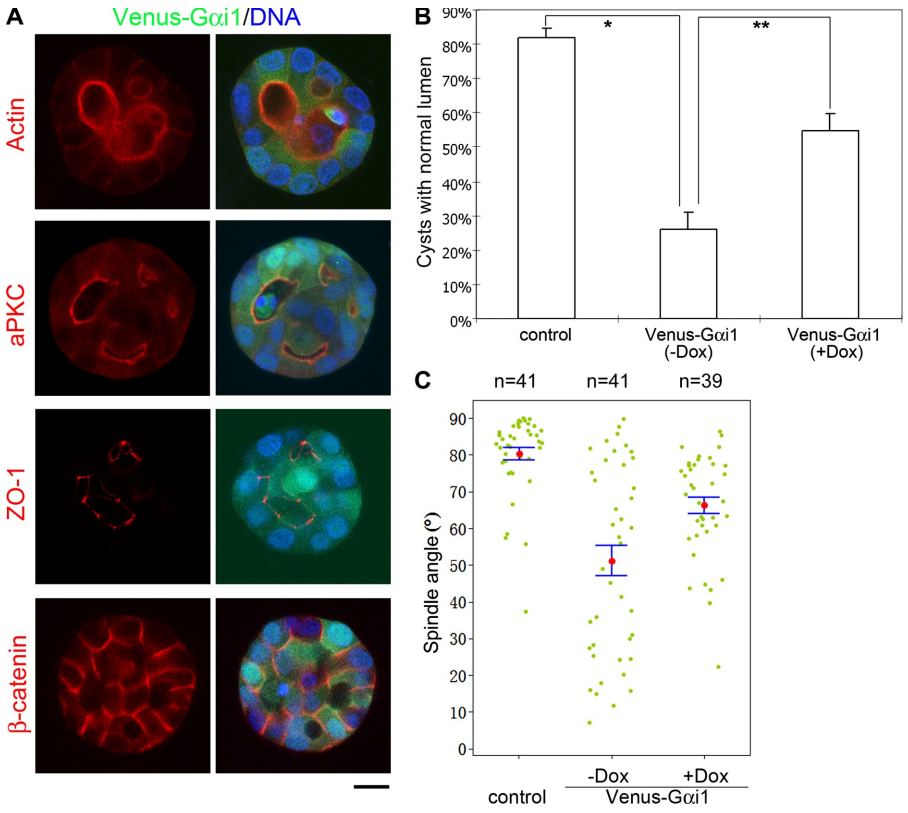

Figure 4. **Overexpression of nonmembrane-bound Gαi1 leads to spindle misorientation and defective cystogenesis.** (A) Overexpression of Venus-Gαi1 induces multiple lumens but does not affect cell polarization during cystogenesis. Stable Tet-Off MDCK cells expressing Venus-Gαi1 were plated in matrigel in the absence of doxycycline for 4 d. Cysts were fixed and immunostained for aPKC, ZO-1, and β-catenin (red). Actin was stained with rhodamine phalloidin (red). DNA was stained with Hoechst 33342 (blue). Single confocal sections through the middle region of the cysts are shown. Merged images are shown on the right. Bar, 20 µm. (B) Quantitation of cysts with single normal lumen from MDCK cells expressing Venus (control) or Venus-Gαi1 in the absence (−Dox) or presence (+Dox) of 20 ng/ml doxycycline. Values are mean ± SD from three independent experiments; $n > 100$ cysts/experiment. *, $P < 0.01$; **, $P < 0.05$. (C) Scatter diagram of metaphase spindle angles in Venus-expressing control cysts or in Venus-Gαi1–expressing cysts grown in the absence (−Dox) or presence (+Dox) of 20 ng/ml doxycycline. Data were presented as in Fig. 3 C.

inducible (Tet-Off) MDCK cell lines expressing N-terminal enhanced YFP (Venus)-tagged Gαi1, which is unable to be post-translationally lipid modified for association with the cell membrane. Cell lines overexpressing Venus only were used as controls. Doxycycline was withdrawn from the culture medium to allow transgene expression for 24 h and cells were then cultured in matrigel for 4 d. Interestingly, whereas most of the control Venus-expressing cells showed normal cystogenesis with the formation of a single central lumen (Fig. 4 B; 81.9 ± 2.9% of cysts formed a single lumen), Venus-Gαi1–expressing cells frequently developed multiple small lumens (Fig. 4, A and B; 26.0 ± 5.1% of cysts formed a single lumen), which was very similar to LGN knockdown cells. Cell polarization appeared normal in Venus-Gαi1 cysts, as revealed by immunostaining of polarity proteins including aPKC, ZO-1, and β-catenin (Fig. 4 A). Overexpression of Venus-Gαi1 also had a profound effect on spindle orientation during cystogenesis (Fig. 4 C; Venus cysts, mean angle = 80.2 ± 1.7°; Venus-Gαi1 cysts [−Dox], mean angle = 51.1 ± 4.1°). Importantly, similar results were obtained from several independent Venus-Gαi1–expressing cell lines (not depicted) and, when doxycycline was kept in the medium to suppress the expression of Venus-Gαi1, significant reductions were observed in abnormal lumen formation (Fig. 4 B; 54.8 ± 4.9% of cysts formed a single lumen in the presence of doxycycline) and spindle misorientation (Fig. 4 C; Venus-Gαi1 cysts [+Dox], mean angle = 66.2 ± 2.3°), suggesting that the cystogenesis defect is attributable to ectopic expression of Venus-Gαi1. The incomplete inhibition of the defects may be due to the leakage of the Tet-Off system. Thus, disrupting the cortical localization of LGN also leads to spindle misorientation and defective cystogenesis.

Dominant-interfering fragments that block LGN interactions with endogenous NuMA or Gα subunits lead to spindle misorientation and defective cystogenesis

While the C terminus of LGN binds Gα, its N terminus interacts with a protein called NuMA (nuclear mitotic apparatus protein) (Du et al., 2001). In fact, LGN forms a complex with NuMA and Gα (Du and Macara, 2004). Is the NuMA–LGN–Gα complex involved in regulating spindle orientation during epithelial morphogenesis? To answer this question, one might propose to knock down NuMA and Gα expression and determine whether a similar phenotype could be observed as LGN knockdown. However, there are several Gα isoforms from the $G\alpha_{i/o}$ family that can bind to LGN (McCudden et al., 2005), and depletion of NuMA leads to spindle organization defect and mitotic catastrophe (Gaglio et al., 1997; Gordon et al., 2001; Kisurina-Evgenieva et al., 2004). Thus, an RNAi approach is not applicable to address our question. We therefore chose a dominant-negative approach by asking whether interfering with the interaction between LGN and Gα or LGN and NuMA would lead to a spindle orientation defect during cystogenesis. Overexpression of the isolated C terminus of LGN, which should compete with endogenous LGN for Gα-GDP binding, is known to have a dominant-negative effect on LGN function (Morin et al., 2007). To interfere with the interaction between endogenous LGN and NuMA, we chose to overexpress a small fragment of NuMA (aa 1818–1921) that contains the LGN-interacting domain but lacks the microtubule-binding and other functional domains of NuMA (Du et al., 2002). Stable Tet-Off MDCK cell lines were isolated expressing Venus-tagged LGN–C terminus (476-CT) or NuMA1818-1921, respectively. As shown in Fig. 5, overexpression of

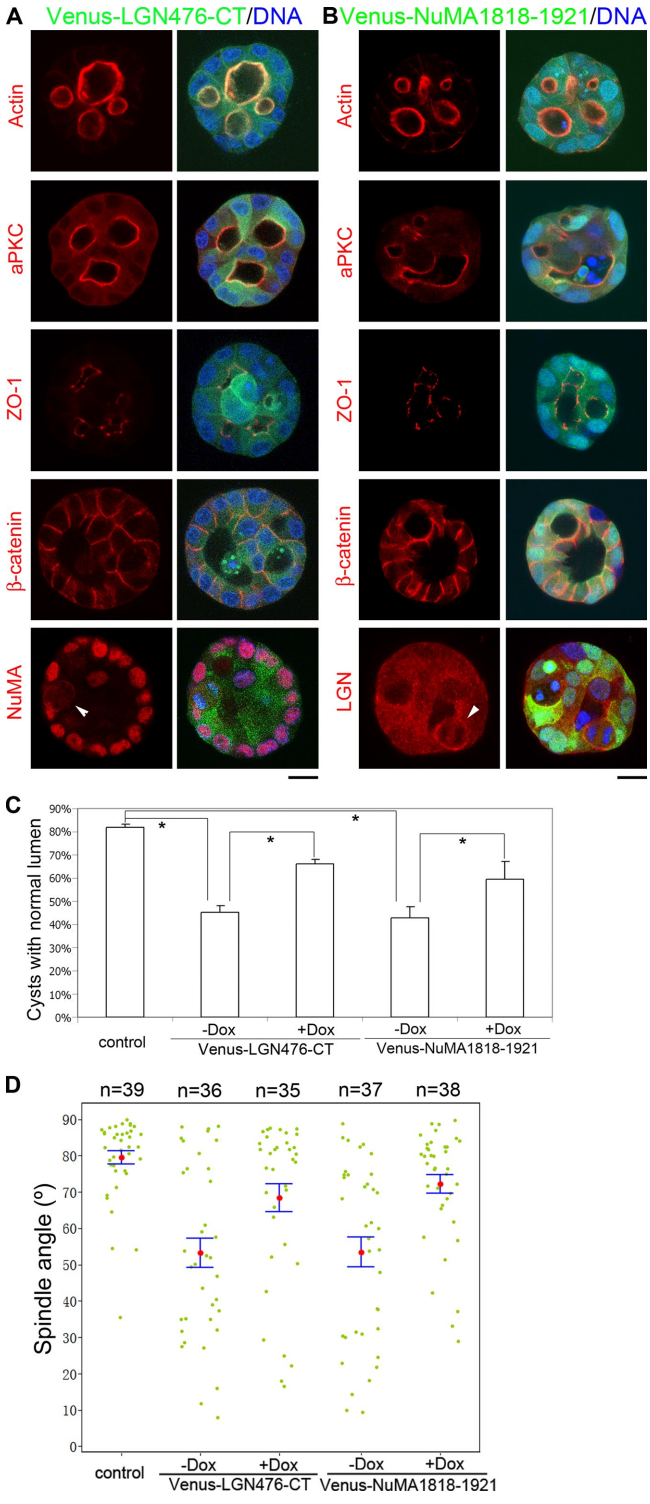

Figure 5. **Overexpression of the C terminus of LGN or the LGN-binding domain of NuMA leads to spindle misorientation and defective cystogenesis.** (A and B) Overexpression of the GoLoco-repeat C terminus of LGN (A) or the LGN-binding domain of NuMA (B) induces multiple lumens but does not affect cell polarization. Stable Tet-Off MDCK cells expressing Venus-LGN476-CT (A) or Venus-NuMA1818-1921 (B) were plated in matrigel in the absence of doxycycline for 4 d. Cysts were fixed and immunostained for aPKC, ZO-1, β-catenin, NuMA, or LGN (red). Actin was stained with rhodamine phalloidin (red, top). DNA was stained with Hoechst 33342 (blue). Single confocal sections through the middle region of the cysts are shown. Merged images are shown on the right. Bars, 20 µm. (C) Quantitation of cysts with single normal lumen from MDCK cells expressing Venus (control), Venus-LGN476-CT, or Venus-NuMA1818-1921 in the absence (−Dox) or presence (+Dox) of 20 ng/ml doxycycline. Values are mean ± SD from three independent experiments; $n > 100$ cysts/experiment. *, $P < 0.01$. (D) Scatter diagram of metaphase spindle angles in cysts expressing Venus (control), Venus-LGN476-CT, or Venus-NuMA1818-1921 in the absence (−Dox) or presence (+Dox) of 20 ng/ml doxycycline. Data were presented as in Fig. 3 C.

either Venus-LGN476-CT or Venus-NuMA1818-1921 resulted in similar, although not as severe, cystogenesis defects as LGN knockdown (Fig. 5, A–C). Abnormal lumen formation was observed in more than 50% of cysts derived from Venus-LGN476-CT and Venus-NuMA1818-1921 expressing cells (Fig. 5 C; 45.1 ± 2.9% and 42.6 ± 5.0% of cysts formed a single lumen, respectively). The localization of aPKC, ZO-1, and β-catenin appeared normal in these cysts (Fig. 5, A and B), suggesting that cell polarization was not affected. Moreover, the localization of endogenous NuMA in Venus-LGN476-CT cells and LGN in Venus-NuMA1818-1921 cells were not obviously altered (Fig. 5, A and B). When we measured spindle axis angle, significant spindle misorientation was observed in Venus-LGN476-CT and Venus-NuMA1818-1921 cysts, compared with that of control cysts (Fig. 5 D, Venus-LGN476-CT cysts [−Dox], mean angle = 53.2 ± 4.0°; Venus-NuMA1818-1921 cysts [−Dox], mean angle = 53.4 ± 4.1°; control cysts, mean angle = 79.4 ± 1.8°). Importantly, the defects in spindle orientation and lumen formation were significantly alleviated when doxycycline was present in the medium to suppress the expression of Venus-LGN476-CT or Venus-NuMA1818-1921 (Fig. 5 C, 66.0 ± 2.0% of Venus-LGN476-CT cysts and 59.5 ± 7.7% of Venus-NuMA1818-1921 cysts formed a single lumen in the presence of doxycycline; Fig. 5 D, Venus-LGN476-CT cysts [+Dox], mean angle = 68.4 ± 3.8°; Venus-NuMA1818-1921 cysts [+Dox], mean angle = 72.1 ± 2.6°). Thus, overexpression of the isolated C terminus of LGN or the LGN-binding domain of NuMA leads to similar phenotype as LGN knockdown, suggesting that LGN functions with Gα and NuMA in regulating spindle orientation in MDCK cells during cystogenesis.

Crumbs-3 serves as an apical targeting vehicle

Our data suggest that LGN may play a critical role in regulating spindle orientation during cystogenesis. It is interesting to observe that LGN localizes to the lateral cortex of dividing cells and is absent from the apical membrane (Fig. 1), which correlates well with spindle orientation during cystogenesis. We reasoned that an approach to validate the role of LGN in directing spindle orientation, and the need of correct spindle orientation for normal lumen formation during cystogenesis, would be to test whether apical mistargeting of LGN would redirect spindle orientation, and if so, what would happen to cystogenesis.

How can we target endogenous LGN to the apical membrane in MDCK cells? Crumbs-3 (Crb3) is a small transmembrane protein that localizes to the apical membrane in polarized MDCK cells (Roh et al., 2003). The C terminus of Crb3 contains a PDZ-binding motif that interacts with the PDZ domain

of Pals1 (Roh et al., 2002). This interaction appears to be important for Crb3 function in cell polarization (Roh et al., 2002, 2003). The apical localization of Crb3, however, is independent of its PDZ-binding motif (Roh et al., 2003). To test whether Crb3 can serve as an apical targeting vehicle, we replaced the C-terminal four amino acids of Crb3 with the coding region of Venus. Stable MDCK cell lines expressing Crb3-Venus fusion protein were established and characterized. When expressed at low or moderate levels, Crb3-Venus localized at the tight junctions and apical membrane in polarized MDCK monolayer (unpublished data). When the cells were grown in matrigel, Crb3-Venus was observed to be exclusively at the apical membrane where it colocalized with F-actin and aPKC (Fig. S3). Cystogenesis appeared to be normal for Crb3-Venus–expressing cells (Fig. S3, Fig. 6 B) and the localization of ZO-1, Pals1, and LGN in these cysts was indistinguishable from that of the control cysts (Fig. S3; Fig. 2). Thus, Crb3 is capable of delivering other proteins to the apical membrane during cystogenesis.

Apical mistargeting of endogenous LGN reverses spindle orientation and leads to severe cystogenesis defects

We showed previously that overexpression of wild-type Gαi1 resulted in enhanced cortical localization of LGN and mitotic chromosome oscillations, suggesting the generation of unbalanced forces on astral microtubules (Du and Macara, 2004). We hypothesized that if we could target Gαi1 to the apical membrane, then endogenous LGN might be recruited to and function at the apical cell cortex. Therefore, a transgene was made in which the wild-type Gαi1 (Gαi1wt) was cloned downstream of, and in-frame with, Crb3-Venus. The transgene was transfected into MDCK cells and stable inducible (Tet-Off) cell lines expressing Crb3-Venus-Gαi1wt fusion protein were isolated. Crb3-Venus-Gαi1wt–expressing cells grew normally under 2D culturing condition in the absence of doxycycline. However, when these cells were plated in matrigel, a profound cystogenesis defect was observed (Fig. 6 A). The defect was similar to but more severe than LGN knockdown cells. Although the majority of Crb3-Venus cells (83.3 ± 1.4%) formed cysts with single lumens, only a small portion of Crb3-Venus-Gαi1wt cells (11.5 ± 4.4%) could do so and the rest developed numerous small lumens (Fig. 6, A and B). A similar phenotype was observed in multiple independent Crb3-Venus-Gαi1wt–expressing cell lines (not depicted). The cystogenesis defect was obvious even when the expression level of Crb3-Venus-Gαi1wt was relatively low; keeping doxycycline in the culture medium significantly inhibited the defect (Fig. 6 B; 57.5 ± 10.1% of cysts formed a single lumen in the presence of doxycycline), suggesting that the defect was caused by ectopic expression of Crb3-Venus-Gαi1. Not surprisingly, the Crb3-Venus-Gαi1wt fusion protein localized exclusively at the apical membrane surrounding those small lumens (Fig. 6 A; Fig. S4 A). Again, it is noteworthy that the localization of polarity determinants aPKC, Pals1, ZO-1, β-catenin, and Dlg1 were not obviously affected in Crb3-Venus-Gαi1wt cysts (Fig. S4 A). Remarkably, endogenous LGN was no longer localized at the lateral cell cortex but recruited to the apical membrane of the cysts in both interphase and mitotic cells (Fig. 6 A). Consistent with our hypothesis of formation of a tripartite NuMA–LGN–Gα complex in vivo (Du and Macara, 2004), endogenous NuMA was also observed to be at the apical membrane in Crb3-Venus-Gαi1wt cysts (Fig. 6 A). We then checked whether apical targeting of Gαi1 affects spindle orientation. Most strikingly, spindle orientation in Crb3-Venus-Gαi1wt cysts was almost completely reversed compared with that of Crb3-Venus cysts (Fig. 6 D, Crb3-Venus cysts, mean angle = 78.3 ± 2.1°; Crb3-Venus-Gαi1wt cysts, mean angle = 13.8 ± 1.7°). The spindle axis in Crb3-Venus-Gαi1wt cells was predominantly parallel to the apical–basal axis, with one spindle pole always facing the apical membrane where Crb3-Venus-Gαi1wt, LGN, and NuMA were localized (Fig. 6, A and D). In Crb3-Venus-Gαi1wt cysts, anaphase cells with chromosomes separating along the apical–basal axis were frequently observed, which was rarely seen in Crb3-Venus cysts (Fig. 6 A and unpublished data). Therefore, without altering cell polarity, apical targeting of Gαi1 reverses mitotic spindle orientation and causes defective cystogenesis.

Are the effects of Crb3-Venus-Gαi1wt mediated through LGN? Although we observed clear apical recruitment of endogenous LGN, we could not rule out the possibility that the effects of Crb3-Venus-Gαi1wt were caused by other Gαi-binding proteins such as the β/γ subunits of heterotrimeric G proteins, which may also affect spindle orientation (Sanada and Tsai, 2005). To address this question, we took advantage of our recent finding that a single amino acid change (asparagine 149 to isoleucine, N149I, GoLoco-insensitive mutant) in Gαi greatly reduces its affinity for LGN GoLoco motifs but preserves all other functional properties of the Gα subunit including binding to G β/γ subunits (Willard et al., 2008). Again, stable Tet-Off MDCK cell lines expressing Crb3-Venus-Gαi1N149I were established and characterized. Consistent with our previous results (Willard et al., 2008), although Crb3-Venus-Gαi1wt was observed to immunoprecipitate endogenous LGN efficiently, Crb3-Venus-Gαi1N149I failed to do so, even when its expression level was much higher than that of Crb3-Venus-Gαi1wt (Fig. S4 C). In a similar fashion to the Crb3-Venus and Crb3-Venus-Gαi1wt fusion proteins, Crb3-Venus-Gαi1N149I localized to the apical membrane during cystogenesis (Fig. 6 C). However, unlike Crb3-Venus-Gαi1wt, apical targeting of the Gαi1N149I point mutant did not affect the localization of endogenous LGN or NuMA (Fig. 6 C). Importantly, cystogenesis appeared normal for Crb3-Venus-Gαi1N149I cells, which were indistinguishable from Crb3-Venus cells in terms of cell polarization (Fig. S4 B), lumen formation (Fig. 6 B; 80.9 ± 4.7% of Crb3-Venus-Gαi1N149I cysts formed a single lumen), and spindle orientation (Fig. 6, C and D; Crb3-Venus-Gαi1N149I cysts, mean angle = 77.5 ± 2.2°). These results suggest that the effect of Crb3-Venus-Gαi1wt on spindle orientation and cystogenesis is likely mediated directly through apical targeting of LGN and NuMA.

The effect of Crb3-Venus-Gαi1wt on cystogenesis relies on cell division

Although we have observed a strong correlation between spindle misorientation and defective cystogenesis, it remains possible

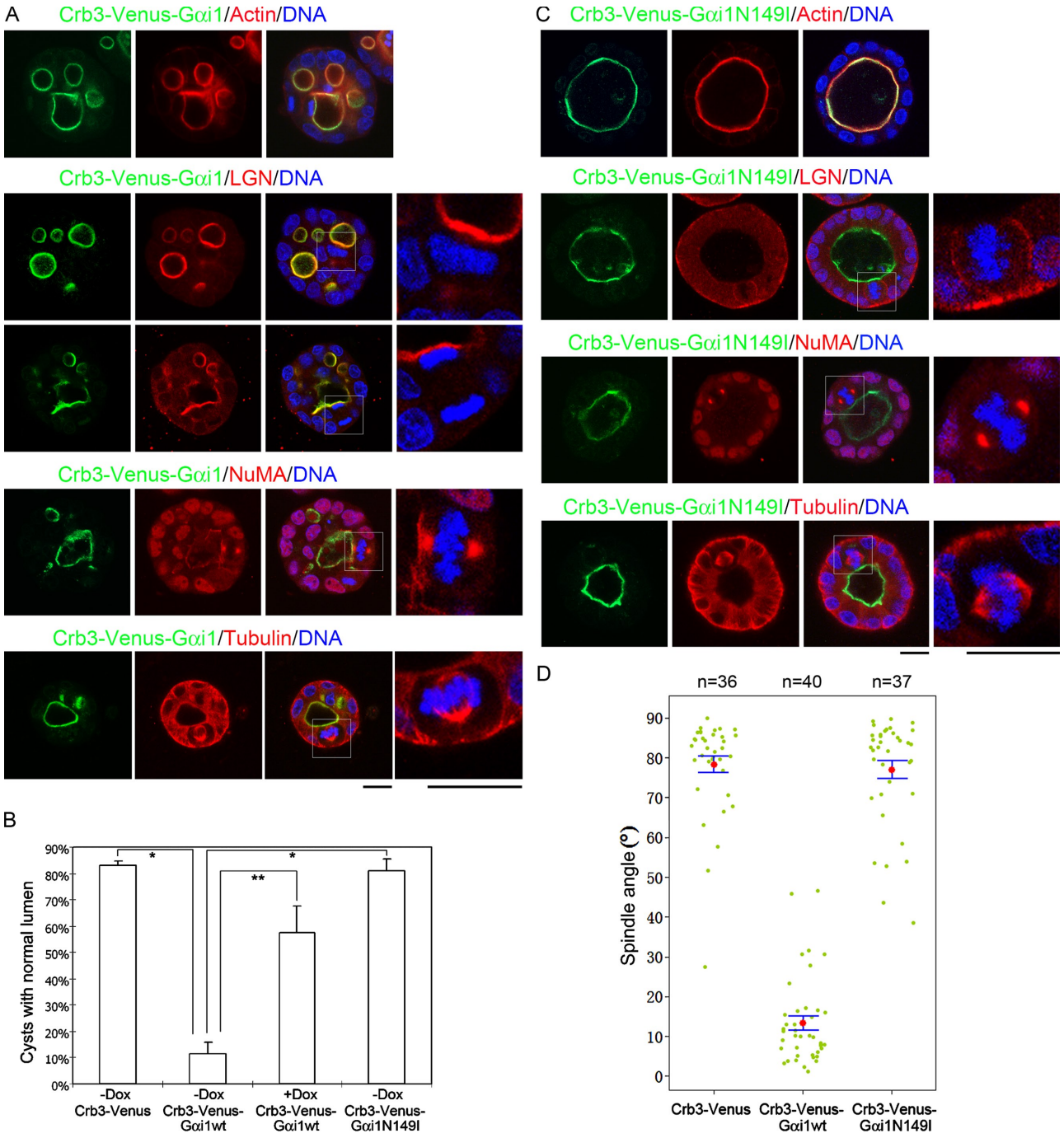

Figure 6. **Forced apical targeting of endogenous LGN reverses spindle orientation and leads to defective cystogenesis.** (A) Stable inducible MDCK cells expressing Crb3-Venus-Gαi1wt were cultured in matrigel in the absence of doxycycline for 4 d. Cysts were fixed and immunostained for LGN, NuMA, and tubulin (red). Actin was stained with rhodamine phalloidin (red, top). DNA was stained with Hoechst 33342 (blue). Single confocal sections through the middle region of the cysts are shown. Enlarged images of highlighted mitotic cells (square boxes) are shown on the right. Bars, 20 µm. (B) Quantitation of cysts with single normal lumen from MDCK cells expressing Crb3-Venus, Crb3-Venus-Gαi1N149I, or Crb3-Venus-Gαi1wt in the absence (−Dox) or presence (+Dox) of 20 ng/ml doxycycline. Values are mean ± SD from three independent experiments; $n > 100$ cysts/experiment. *, $P < 0.001$; **, $P < 0.01$. (C) Apical targeting of the GoLoco-insensitive Gαi1 mutant (Gαi1N149I) does not affect cystogenesis, localization of LGN and NuMA, or mitotic spindle orientation. Stable MDCK cells expressing Crb3-Venus-Gαi1N149I were plated in matrigel in the absence of doxycycline for 4 d and analyzed as in A. (D) Scatter diagram of metaphase spindle angles in cysts expressing Crb3-Venus, Crb3-Venus-Gαi1wt, or Crb3-Venus-Gαi1N149I. Data were presented as in Fig. 3 C.

that the abnormal cystogenesis is caused by other morphogenetic events, such as cell movement or cell–cell interactions. We reasoned that if spindle misorientation and subsequent mispositioning of the cleavage plane contribute to abnormal lumen formation, then inhibition of cell proliferation or cell division would block defective cystogenesis caused by spindle misorientation. To test this hypothesis, we took advantage of our Tet-Off cell line where Crb3-Venus-Gαi1wt expression and spindle

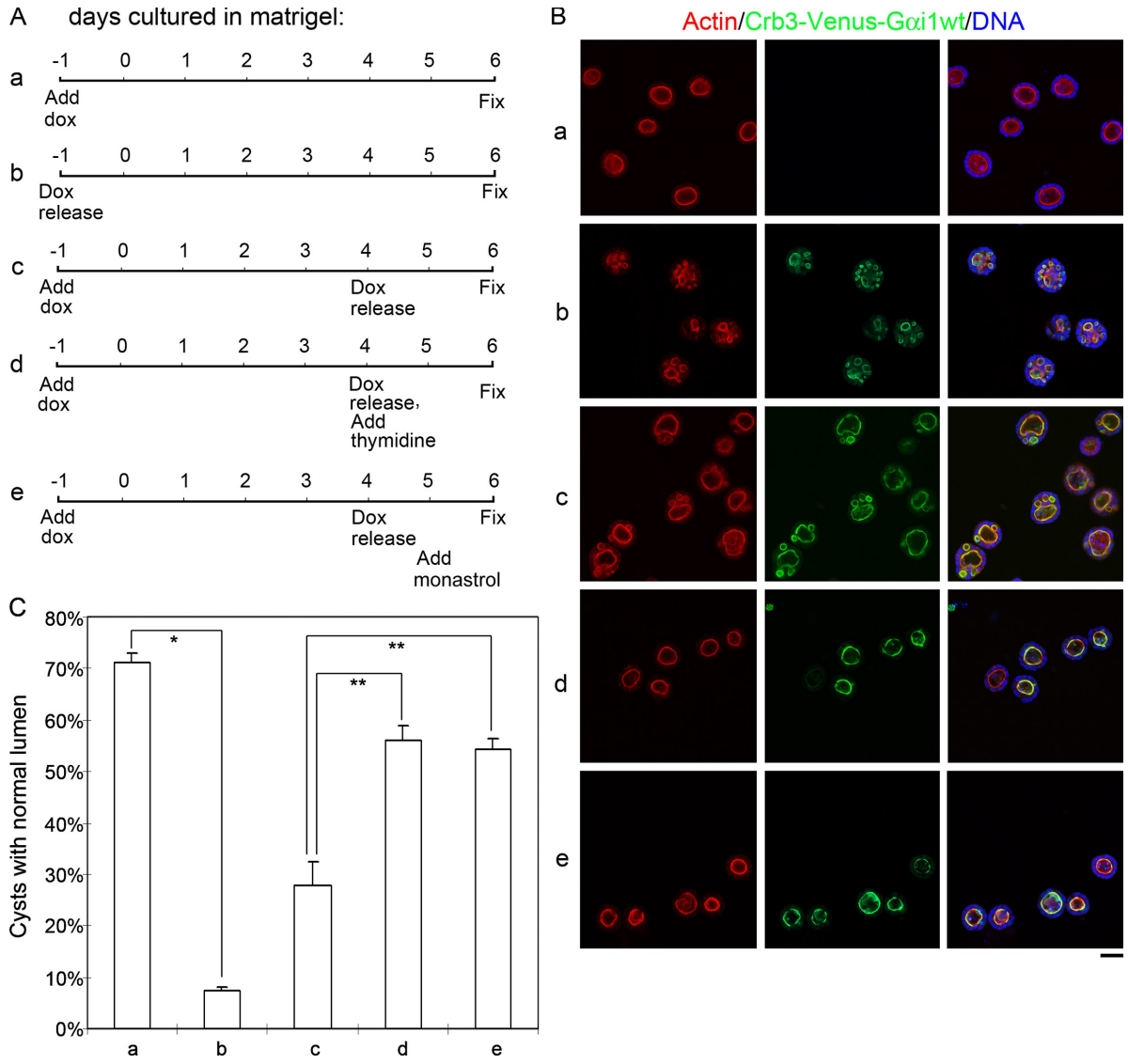

Figure 7. **Cell proliferation and cell division are required for Crb3-Venus-Gαi1wt–induced defective cystogenesis.** (A) Schematics of experimental design. Stable Tet-Off MDCK cells expressing Crb3-Venus-Gαi1wt were cultured as indicated. dox, doxycycline. (B) Representative images of cysts grown for 6 d under different experimental conditions as depicted in A. Actin was stained with rhodamine phalloidin (red). DNA was stained with Hoechst 33342 (blue). Single confocal sections through the middle region of the cysts are shown. Merged images are shown on the right. Bar, 50 µm. (C) Quantitation of cysts with single lumen from MDCK cells expressing Crb3-Venus-Gαi1wt at d 6 under different experimental conditions as depicted in A. Values are mean ± SD from three independent experiments; $n > 100$ cysts/experiment. *, $P < 0.001$; **, $P < 0.01$.

misorientation could be induced by doxycycline withdrawal (Fig. 7 A). Cells were grown in the presence of doxycycline for 4 d to allow normal lumen development. Then doxycycline was withdrawn from the culture media to induce the expression of Crb3-Venus-Gαi1wt. Unlike cysts that were kept in doxycycline (Fig. 7, B and C; group [a], 71.2 ± 1.9% of cysts formed a single lumen), 2 d after doxycycline withdrawal a large portion of the cysts had developed multiple small lumens surrounding the preformed central lumen (Fig. 7, B and C; group [c], 27.8 ± 4.6% of cysts formed a single lumen). We then added thymidine (2 mM) to the culture media right after doxycycline withdrawal. Thymidine treatment of MDCK cells resulted in significant inhibition of cell proliferation and reduced mitotic index (Fig. S5, A and B). No obvious cell death was observed after 48 h of treatment and the expression level of Crb3-Venus-Gαi1wt was comparable to that of untreated cells (Fig. 7 B; Fig. S5 C). However, thymidine treatment significantly inhibited abnormal lumen formation (Fig. 7, B and C; group [d], 56.2 ± 2.8% of cysts formed a single lumen), suggesting that the effect of Crb3-Venus-Gαi1wt on cystogenesis requires cell proliferation.

To test more specifically whether cell division is required for Crb3-Venus-Gαi1wt–induced abnormal lumen formation, we performed similar experiments by adding monastrol after doxycycline withdrawal. Monastrol is a potent inhibitor of mitosis-specific kinesin Eg5, which is required for centrosome separation and bipolar spindle formation (Mayer et al., 1999). We used a moderate concentration of monastrol (50 µM) to avoid mitotic catastrophe after prolonged treatment (24 h). Interestingly, monastrol treatment also resulted in a reduction of

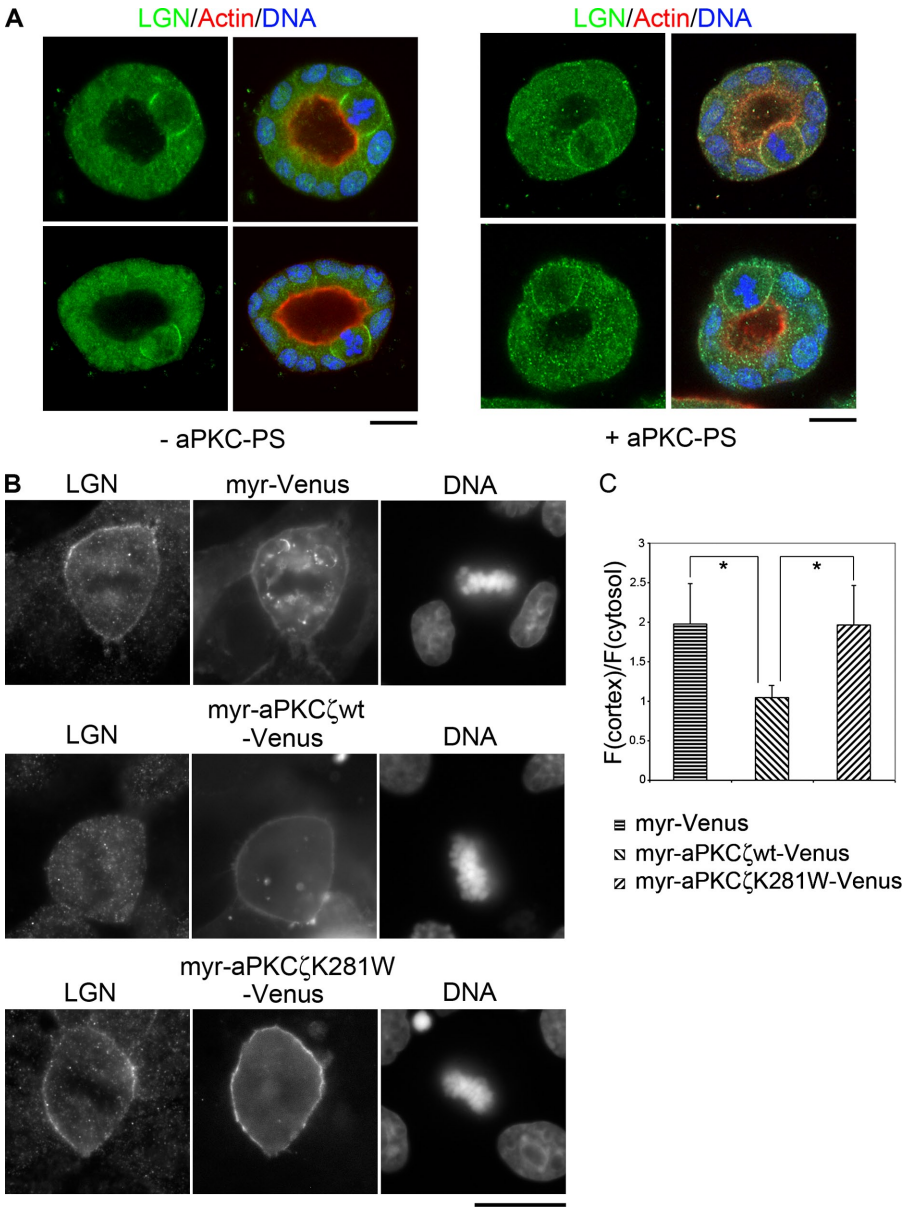

Figure 8. **aPKC activity prevents apical localization of LGN during cystogenesis.** (A) Inhibition of aPKC activity leads to apical diffusion of LGN. MDCK II cells were plated in matrigel for 3 d to allow cystogenesis. Cysts were treated with aPKC-PS (40 µM final concentration) for 24 h or left untreated. Treated (+aPKC-PS) or untreated (−aPKC-PS) cysts were then fixed and immunostained for LGN (green). Actin was stained with rhodamine phalloidin (red). DNA was stained with Hoechst 33342 (blue). Single confocal sections through the middle region of the cysts are shown. Merged images are shown on the right. Bars, 20 µm. (B) Overexpression of active PKC-ζ inhibits cortical localization of LGN. MDCK cells were transfected with pK-myr-Venus, pK-myr-aPKCζwt-Venus, or pK-myr-aPKCζK281W-Venus and cultured for 24 h. Cells were fixed and immunostained with anti-LGN antibody (left). DNA was stained with Hoechst 33342 (right). Bar, 20 µm. (C) Quantitation of the relative fluorescence intensity of cortical LGN in cells expressing myr-Venus, myr-aPKCζwt-Venus, or myr-aPKCζK281W-Venus. Fluorescence intensities at the cortex and 10 pixels away at the cytosol were refered to as F(cortex) and F(cytosol), respectively. The ratio of F(cortex)/F(cytosol) was collected for each group of cells and analyzed. Values are mean ± SD from three independent experiments; $n > 10$ cells/experiment. *, $P < 0.0001$.

multiple lumen formation caused by ectopic Crb3-Venus-Gαi1wt expression (Fig. 7, B and C; group [e], 54.2 ± 2.3% of cysts formed a single lumen), although mitotic cells were frequently observed in treated cysts.

Importantly, thymidine or monastrol treatment did not affect the apical recruitment of endogenous LGN by Crb3-Venus-Gαi1wt (Fig. S5 D), and the distribution of polarity proteins was not obviously altered within the time frame of treatment (not depicted). These results strongly suggest that it is the misoriented cell division that contributes to the observed defective cystogenesis.

The normal apical exclusion of LGN appears to be mediated by aPKC

Our data implicate the normal localization pattern of LGN as important for directing spindle orientation to be orthogonal to the apical–basal axis during cystogenesis. LGN is normally absent from the apical cell cortex during mitosis and forced apical localization of LGN reverses spindle orientation (Fig. 1, Fig. 6). Then what is the molecular mechanism that prevents the apical localization of LGN during cystogenesis? A good candidate that may serve to exclude LGN from the apical cell cortex would be aPKC, which localizes at the apical cell membrane during cystogenesis. To test whether aPKC is involved in regulating LGN localization during cystogenesis, we plated normal MDCK cells in matrigel for 3 d to allow cyst formation. aPKC-PS, a myristoylated pseudosubstrate of aPKC, was added in the culture medium to inhibit aPKC activity. Treated and untreated cysts were then fixed and stained with anti-LGN antibodies. As shown in Fig. 8 A, in control cysts, LGN was enriched at the lateral cortex of mitotic cells. However, in cysts treated with aPKC-PS, the lateral staining of LGN appeared to be weaker and apical localization of LGN was frequently observed. However, due to the adverse effect of aPKC-PS on cystogenesis (many cysts collapsed after the treatment), we were not able

to address the effect of aPKC-PS on spindle orientation under our experimental conditions.

To further test whether aPKC can affect LGN localization, we overexpressed a myristoylated (and thus activated) form of aPKC-ζ (myr-aPKCζwt-Venus) in MDCK cells. Although overexpression of myristoylated venus (myr-Venus) did not affect the cortical localization of LGN, overexpression of myr-aPKCζwt-Venus resulted in significant reduction of cortical LGN staining in mitotic cells (Fig. 8, B and C). The kinase activity appeared to be required for the effect of aPKC on LGN localization because overexpression of a myristoylated, kinase-deficient mutant of aPKCζ (myr-aPKCζK281W-Venus) did not obviously affect LGN localization (Fig. 8, B and C). Taken together, aPKC is capable of inhibiting the cortical localization of LGN and may function to exclude LGN from the apical membrane during cystogenesis.

Discussion

Recently, the molecular mechanisms of spindle orientation in symmetrically dividing mammalian cells have been studied in 2D culturing systems (Théry et al., 2007; Toyoshima and Nishida, 2007; Toyoshima et al., 2007; den Elzen et al., 2009; Mitsushima et al., 2009). However, due to the nature of the 2D system, the observed spindle orientation defects, although statistically significant, are subtle and do not apparently cause obvious biological consequence. Organotypic 3D culture of epithelial cells in vitro recapitulates many aspects of epithelial morphogenesis in vivo (O'Brien et al., 2002; Debnath and Brugge, 2005). Here, using a 3D cultured MDCK cell system, we demonstrate that spindle orientation is indeed critical for epithelial morphogenesis. We identified LGN as an important spindle orientation determinant in symmetrically dividing MDCK cells. Without an obvious effect on cell polarization, depletion of LGN expression and disruption of the cortical localization of LGN both result in spindle misorientation and defective cystogenesis.

How does LGN regulate spindle orientation during cystogenesis? Our data suggest that the interaction between LGN and Gα appears to be required for LGN function. On the one hand, Gα may help to bring LGN to the cell cortex. On the other hand, the binding of Gα to LGN may alter the conformation of LGN and activate LGN at the cell cortex (Du and Macara, 2004; Nipper et al., 2007). LGN may also function through its interaction with NuMA, a microtubule-binding protein that appears to be linked to cytoplasmic dynein (Merdes et al., 1996; Du et al., 2001). Indeed, interfering with the interaction between endogenous LGN and Gα, or LGN and NuMA resulted in spindle misorientation and defective cystogenesis. We conclude that the evolutionarily conserved NuMA–LGN–Gα complex may function in directing spindle orientation during cystogenesis of MDCK cells. Using Crb3 as an apical targeting vehicle, we showed that apical targeting of wild-type Gαi1, but not the GoLoco-insensitive Gαi1, resulted in apical recruitment of endogenous LGN as well as NuMA and complete reversion of spindle orientation, suggesting that the NuMA–LGN–Gα complex is indeed capable of directing spindle orientation in mammalian cells. Importantly, the artificial reversion of spindle orientation resulted in a similar cystogenesis defect as LGN knockdown, further supporting the notion that LGN is involved in regulating spindle orientation during cystogenesis. By manipulating the inducible cell lines and by applying chemical inhibitors, we show that the effect of ectopic Crb3-Venus-Gαi1wt expression on cystogenesis requires cell division, suggesting further that the defective cystogenesis was caused by misoriented cell division. Recently, it was shown that in *Drosophila*, the interaction between Pins (the fly homologue of LGN) and Discs large (Dlg) is required for Pins in regulating spindle orientation (Siegrist and Doe, 2005; Johnston et al., 2009). We do not know yet whether mammalian Dlg homologues are involved in LGN function in directing spindle orientation. However, in Crb3-Venus-Gαi1wt cysts in which endogenous LGN was recruited to the apical membrane and spindle orientation was reversed, we did not observe clear apical recruitment of Dlg1 (Fig. S4 and unpublished data), suggesting that Dlg1 may not be required for LGN–Gαi1 to direct spindle orientation in MDCK cells. How the NuMA–LGN–Gα complex interacts with astral MTs to direct spindle orientation at the molecular level is still elusive. The inducible Crb3-Venus-Gαi1wt cells should provide a robust system for further dissecting the molecular mechanisms of spindle orientation in mammalian cells.

During asymmetric cell division of stem/progenitor cells, cell polarization is tightly coupled to spindle orientation (Betschinger and Knoblich, 2004; Roegiers and Jan, 2004; Siller and Doe, 2009). Interestingly, we show here that in symmetrically dividing MDCK cells during cystogenesis, spindle orientation may also be affected by cell polarization. The fact that activated aPKC is able to dissociate LGN from the cell cortex, and that inhibition of aPKC activity results in apical diffusion of LGN is intriguing. We propose that apical localization of aPKC during cystogenesis is critical for restricting LGN to the lateral cell cortex and thus directing spindle orientation to be perpendicular to the apical–basal axis. In line with our hypothesis, overexpression of wild-type or dominant-negative aPKCλ in MDCK cells is seen to result in similar cystogenesis defects as LGN depletion (Horikoshi et al., 2009). How aPKC excludes LGN from the apical cell cortex during cystogenesis is not clear. It is possible that aPKC may directly phosphorylate LGN and lead to its dissociation from the apical membrane. Another possibility is that aPKC may function to exclude the apical localization of another protein that is required to anchor LGN at the cell cortex. Candidate proteins that may help the cortical localization of LGN include Lgl (Lethal giant larvae) and Dlg, which have been shown to be direct LGN binding partners (Sans et al., 2005; Yasumi et al., 2005). In *Drosophila* neuroblasts, aPKC phosphorylates and excludes Lgl from the apical cell cortex and contributes to the basal localization of cell fate determinants (Betschinger and Knoblich, 2004). However, in asymmetrically dividing neuroblasts, aPKC and Pins colocalize at the apical cell cortex (Betschinger and Knoblich, 2004). We believe that the colocalization of aPKC and Pins might be neuroblast specific. It may be attributable to neuroblast-specific expression of Inscuteable, which links Pins to apically localized Bazooka (Roegiers and Jan, 2004). We showed that Crb3-Venus-Gαi1wt

could recruit endogenous LGN to the apical membrane where aPKC was still present (Fig. 6 A; Fig. S4), suggesting that excess Gαi1wt could also counteract the dissociation activity of aPKC on the cortical localization of LGN. Further experiments are required to elucidate the mechanism by which aPKC regulates the localization of LGN.

We found that the major cystogenesis defect resulting from spindle misorientation in MDCK cells was the formation of multiple lumens. A similar phenotype had been observed previously and was attributed to defects in cell polarization or apical vesicle transport (Martin-Belmonte et al., 2007; Bryant and Mostov, 2008; Horikoshi et al., 2009). However, by careful examination of multiple polarity proteins, we can exclude an obvious cell polarity defect in multi-luminal cysts derived from misoriented cell division. Our results are consistent with recent studies in 3D cultured Caco-2 cells, in which Cdc42 knockdown did not cause an apical–basal polarization defect but resulted in spindle misorientation and the formation of multiple lumens (Jaffe et al., 2008). As a central player in cell polarization, aPKC is closely linked to many other polarity proteins such as Cdc42. The potential link between aPKC and LGN, and thus spindle orientation, suggests that it would be interesting to reexamine those multi-luminal cysts to determine whether LGN localization and spindle orientation are perturbed.

Materials and methods

Reagents

Rabbit anti-LGN and rabbit anti-NuMA antibodies were described previously (Du and Macara, 2004). The following antibodies were also used: mouse anti–α-tubulin (Sigma-Aldrich), mouse anti–ZO-1(Invitrogen), mouse anti–β-catenin (BD), mouse anti-Dlg1 (Santa Cruz Biotechnology, Inc.), rabbit anti-aPKC (Santa Cruz Biotechnology, Inc.), rabbit anti-Pals1(a gift from Dr. Ian Macara, University of Virginia, Charlottesville, VA), rabbit anti-GFP (Torry Pines Biolabs); and secondary Alexa 488, Alexa 594, Alexa 660, Alexa 680 (Invitrogen), and IRDye800 (Rockland) conjugated goat anti–mouse or rabbit antibodies. Hoechst 33342 (Invitrogen) was used for DNA staining and rhodamine-conjugated phalloidin (Invitrogen) was used to visualize F-actin. Myristoylated PKCζ pseudo-substrate (aPKC-PS) was purchased from Invitrogen.

Cell culture and stable cell lines

MDCK cells were cultured in DME supplemented with 10% fetal calf serum and penicillin/streptomycin (100 IU/ml and 100 mg/ml, respectively) at 37°C in a humidified 5% CO_2 atmosphere.

Stable Tet-Off inducible MDCK cell lines were generated as described previously (Du et al., 2001). In brief, an enhanced YFP (Venus) was cloned into pTRE2Hyg vector (Takara Bio Inc.). cDNAs encoding human NuMA1818-1921, LGN-CT (476–677), and Gαi1 were inserted downstream of, and in-frame with, Venus, respectively. These plasmids were transfected into MDCK T23 cells, which express the tetracycline-repressible transactivator. Cells were passaged 24 h after transfection onto P-150 plates in medium containing 200 ug/ml hygromycin B and 20 ng/ml doxycycline. After selection for 7–10 d, surviving colonies were isolated using cloning rings (Thermo Fisher Scientific), and the expression of Venus fusion proteins was assessed by immunofluorescence microscopy and Western blotting after removal of doxycycline.

For inducible MDCK cell lines expressing Crb3-Venus, Crb3-Venus-Gαi1wt, and Crb3-Venus-Gαi1N149I, Crb3 cDNA (a gift from Dr. Ben Margolis, University of Michigan, Ann Arbor, MI; aa 1–116) was first cloned in pTRE2Hyg vector. Venus was then cloned downstream of, and in-frame with, Crb3 to make pTRE2Crb3-Venus. cDNAs encoding wild-type or the N149I mutant Gαi1 were inserted in pTRE2Crb3-Venus to generate pTRE2Crb3-Venus-Gαi1wt and pTRE2Crb3-Venus-Gαi1N149I. These plasmids were transfected into MDCK T23 cells and stable clones were isolated as described above.

The 3D culture of MDCK cells in matrigel was performed as described previously for MCF10A cells (Debnath et al., 2003). In brief, MDCK cells were trypsinized and resuspended to single cell suspension of 4×10^4 cells/ml in 2% matrigel (BD). 400 µl of cells were plated in each well of 8-well Lab-Tek II chamber slides (Thermo Fisher Scientific) precovered with matrigel (30 µl per well). Cells were fed every 2 d and grown for 3–6 d as indicated. For drug treatment, 2 mM thymidine or 50 µM monastrol (Sigma-Aldrich) was used.

Lentivirus production and infection

pLentiLox3.7 (pLL3.7) vector was used for lentivirus-mediated stable knockdown of LGN in MDCK cells. In brief, long oligos containing target sequences were cloned downstream of the U6 promoter in pLL3.7 to generate specific RNAi vectors. Once sequence verified and efficiency tested by transient transfection, the RNAi vectors were cotransfected with the lenti-packaging mix (Invitrogen) into HEK293 cells, and the pseudo-virus containing supernatant was collected 48 h after transfection. Virus supernatant was used to infect MDCK cells cultured in 12-well plates. 24 h after infection, the cells were passaged onto P-100 plates and transduced clones (based on virus-mediated expression of GFP) were marked and isolated using cloning rings 1 wk later. The knockdown efficiency was analyzed by Western blot and immunostaining of LGN. Target sequences for LGN were 5′-GGTCTAAGCTACAGCACAAAT-3′ (LGN-KD1) and 5′-GCAGCTGAAAGAAGAGCATAT-3′ (LGN-KD2).

Western blotting and immunoprecipitation

Cells were washed with cold PBS and collected in cell lysis buffer (25 mM Hepes, pH 7.4, 150 mM NaCl, 0.5% Triton X-100, 0.5 mM EDTA, 5 mM $MgCl_2$, 1 mM DTT, 1 mM PMSF, 10 µg/ml leupeptin, and 20 ug/ml aprotinin). Cell debris was removed by centrifugation at 14,000 rpm for 20 min at 4°C. SDS sample buffer was added to equal amounts of cell lysate and proteins were separated by SDS-PAGE, transferred onto nitrocellulose membranes, and analyzed with the antibodies indicated in the text. Immunoprecipitation was performed as described previously (Du and Macara, 2004). In brief, Stable Tet-Off inducible MDCK cells expressing Crb3-Venus-Gαi1wt and Crb3-Venus-Gαi1N149I were cultured in medium without doxycycline for 2 d and lysed in cell lysis buffer. Equal amounts of cell lysate were incubated with 2 µg anti-GFP antibody at 4°C for 1 h, GammaBind-Plus Sepharose (GE Healthcare), blocked with 5% BSA (Sigma-Aldrich), were added, and the mixture was incubated for 45 min at 4°C. Immunoprecipitates were washed four times with cell lysis buffer and separated by SDS-PAGE. Proteins were transferred to nitrocellulose membrane and detected using anti-LGN and anti-GFP antibodies.

Immunofluorescence microscopy

MDCK cells grown on coverglass or chamber slides were fixed with 4% paraformaldehyde in PBS and permeabilized with 0.5% Triton X-100 in PBS. Fixed cells were blocked with 10% normal goat serum/1%BSA in PBS for 1 h, and then incubated for 1 h with the following primary antibodies: anti-LGN (1:200), anti-NuMA (1:500), anti–α-tubulin (1:1,000), anti–ZO-1 (1:1,000), anti-aPKC (1:100), anti–β-catenin (1:1,000), anti–Pals-1 (1:200), and anti-Dlg1 (1:100). Cells were then washed and incubated for 1 h with DNA stain Hoechst 33342 and goat anti–mouse or anti–rabbit secondary antibodies coupled to Alexa 488 or Alexa 594 (Invitrogen). Cysts formed in matrigels were processed in a similar manner except that the incubation time for each procedure was prolonged. Epifluorescent images were taken on an inverted microscope (TE2000; Nikon) using a 60×/1.2 NA oil-immersion objective. Confocal images were captured on a confocal microscope (510 LSM; Carl Zeiss, Inc.) using a Plan Apochromat 63×/1.4 NA or Plan Neofluar 25×/0.8 NA oil objectives (Carl Zeiss, Inc.) and analyzed using the LSM Image Examiner and Adobe Photoshop software. To quantitate cysts with normal lumens, more than 100 cysts were analyzed per experiment. Cysts with actin staining at the apical surface of cells surrounding a single lumen were identified as cysts with normal lumens. Standard deviation was calculated, and statistical significance was determined by Student's *t* test.

Measurement of spindle angle

The measurement of spindle angle was performed as described previously for Caco-2 cysts (Jaffe et al., 2008) with the following modifications (see Fig. 3 B for schematic). Cysts grown for 3–4 d were fixed and stained with anti–α-tubulin antibody (Fig. 3 B, green) and Hoechst 33342 (Fig. 3 B, blue). Confocal images of metaphase or anaphase cells in the middle region of the cysts were collected. A line was drawn using ImageJ (National Institutes of Health, Bethesda, MD) to connect the two spindle poles (Fig. 3 B,

thick black lines). Another line was drawn from the centroid of the apical domain to the midpoint of the spindle axis (Fig. 3 B, thin black lines) and the acute angle (Fig. 3 B, red) between the two lines was analyzed.

Measurement of the relative fluorescence intensity of cortical LGN

The myristoylation signal from v-Src was cloned in pRK5 under the control of the CMV promoter. The coding sequence of Venus was cloned downstream of and in-frame with the myristoylation signal to make pK-myr-Venus. cDNAs encoding wild-type or K281W mutant of mouse PKCζ were inserted between and in-frame with the myristoylation signal and Venus to generate pK-myr-aPKCζwt-Venus and pK-myr-aPKCζK281W-Venus. These plasmids were transfected into MDCK II cells and the cells were fixed 24 h after transfection. Fixed cells were stained with anti-LGN primary antibody and Alexa 594–conjugated goat anti–rabbit secondary antibody. DNA was stained with Hoechst 33342. Images of transfected mitotic cells were taken on the Nikon TE2000 microscope. To compare the relative fluorescence intensity of cortical LGN, a 30-pixel line was draw across the cell border using MetaMorph software (MDS Analytical Technologies). The Line Scan function of MetaMorph was used to reveal the relative fluorescence intensity across the line. Fluorescence intensities at the cortex and 10 pixels away at the cytosol were refered to as F(cortex) and F(cytosol), respectively. The ratio of F(cortex)/F(cytosol) was collected for each group of cells and analyzed. Standard deviation was calculated, and statistical significance was determined by Student's *t* test.

Online supplemental material

Fig. S1 shows that LGN knockdown does not alter cell proliferation or the morphology of mitotic spindle in MDCK cells. Fig. S2 shows that LGN knockdown alters spindle orientation and induces multiple lumens, but does not affect cell polarization. Fig. S3 shows that Crumbs3 targets Venus to the apical membrane during cystogenesis. Fig. S4 shows that apical targeting of Gαi1wt or Gαi1N149I does not affect cell polarization during cystogenesis. Fig. S5 shows the effects of thymidine or monastrol treatment on Crb3-venus-Gαi1wt cells. Online supplemental material is available at http://www.jcb.org/cgi/content/full/jcb.200910021/DC1.

We are grateful to Dr. Ian G. Macara, Dr. Ben Margolis, and Dr. Duane A. Compton for sharing valuable reagents. We also thank Dr. Lin Mei for critical reading of the manuscript.

This work was supported by National Institutes of Health grants to Q. Du (GM079506) and D. Siderovski (GM074268), and an American Cancer Society grant to Q. Du (RSG0717601CSM).

Submitted: 5 October 2009
Accepted: 25 March 2010

References

Ahringer, J. 2003. Control of cell polarity and mitotic spindle positioning in animal cells. *Curr. Opin. Cell Biol.* 15:73–81. doi:10.1016/S0955-0674(02)00018-2

Baena-López, L.A., A. Baonza, and A. García-Bellido. 2005. The orientation of cell divisions determines the shape of *Drosophila* organs. *Curr. Biol.* 15:1640–1644. doi:10.1016/j.cub.2005.07.062

Bernard, M.L., Y.K. Peterson, P. Chung, J. Jourdan, and S.M. Lanier. 2001. Selective interaction of AGS3 with G-proteins and the influence of AGS3 on the activation state of G-proteins. *J. Biol. Chem.* 276:1585–1593. doi:10.1074/jbc.M005291200

Betschinger, J., and J.A. Knoblich. 2004. Dare to be different: asymmetric cell division in *Drosophila, C. elegans* and vertebrates. *Curr. Biol.* 14:R674–R685. doi:10.1016/j.cub.2004.08.017

Bowman, S.K., R.A. Neumüller, M. Novatchkova, Q. Du, and J.A. Knoblich. 2006. The *Drosophila* NuMA Homolog Mud regulates spindle orientation in asymmetric cell division. *Dev. Cell.* 10:731–742. doi:10.1016/j.devcel.2006.05.005

Bryant, D.M., and K.E. Mostov. 2008. From cells to organs: building polarized tissue. *Nat. Rev. Mol. Cell Biol.* 9:887–901. doi:10.1038/nrm2523

Colombo, K., S.W. Grill, R.J. Kimple, F.S. Willard, D.P. Siderovski, and P. Gönczy. 2003. Translation of polarity cues into asymmetric spindle positioning in *Caenorhabditis elegans* embryos. *Science.* 300:1957–1961. doi:10.1126/science.1084146

Couwenbergs, C., J.C. Labbé, M. Goulding, T. Marty, B. Bowerman, and M. Gotta. 2007. Heterotrimeric G protein signaling functions with dynein to promote spindle positioning in C. elegans. *J. Cell Biol.* 179:15–22. doi:10.1083/jcb.200707085

Debnath, J., and J.S. Brugge. 2005. Modelling glandular epithelial cancers in three-dimensional cultures. *Nat. Rev. Cancer.* 5:675–688. doi:10.1038/nrc1695

Debnath, J., S.K. Muthuswamy, and J.S. Brugge. 2003. Morphogenesis and oncogenesis of MCF-10A mammary epithelial acini grown in three-dimensional basement membrane cultures. *Methods.* 30:256–268. doi:10.1016/S1046-2023(03)00032-X

den Elzen, N., C.V. Buttery, M.P. Maddugoda, G. Ren, and A.S. Yap. 2009. Cadherin adhesion receptors orient the mitotic spindle during symmetric cell division in mammalian epithelia. *Mol. Biol. Cell.* 20:3740–3750. doi:10.1091/mbc.E09-01-0023

Du, Q., and I.G. Macara. 2004. Mammalian Pins is a conformational switch that links NuMA to heterotrimeric G proteins. *Cell.* 119:503–516. doi:10.1016/j.cell.2004.10.028

Du, Q., P.T. Stukenberg, and I.G. Macara. 2001. A mammalian Partner of inscuteable binds NuMA and regulates mitotic spindle organization. *Nat. Cell Biol.* 3:1069–1075. doi:10.1038/ncb1201-1069

Du, Q., L. Taylor, D.A. Compton, and I.G. Macara. 2002. LGN blocks the ability of NuMA to bind and stabilize microtubules. A mechanism for mitotic spindle assembly regulation. *Curr. Biol.* 12:1928–1933. doi:10.1016/S0960-9822(02)01298-8

Gaglio, T., M.A. Dionne, and D.A. Compton. 1997. Mitotic spindle poles are organized by structural and motor proteins in addition to centrosomes. *J. Cell Biol.* 138:1055–1066. doi:10.1083/jcb.138.5.1055

Gordon, M.B., L. Howard, and D.A. Compton. 2001. Chromosome movement in mitosis requires microtubule anchorage at spindle poles. *J. Cell Biol.* 152:425–434. doi:10.1083/jcb.152.3.425

Grill, S.W., and A.A. Hyman. 2005. Spindle positioning by cortical pulling forces. *Dev. Cell.* 8:461–465. doi:10.1016/j.devcel.2005.03.014

Grill, S.W., J. Howard, E. Schäffer, E.H. Stelzer, and A.A. Hyman. 2003. The distribution of active force generators controls mitotic spindle position. *Science.* 301:518–521. doi:10.1126/science.1086560

Horikoshi, Y., A. Suzuki, T. Yamanaka, K. Sasaki, K. Mizuno, H. Sawada, S. Yonemura, and S. Ohno. 2009. Interaction between PAR-3 and the aPKC-PAR-6 complex is indispensable for apical domain development of epithelial cells. *J. Cell Sci.* 122:1595–1606. doi:10.1242/jcs.043174

Izumi, Y., N. Ohta, K. Hisata, T. Raabe, and F. Matsuzaki. 2006. *Drosophila* Pins-binding protein Mud regulates spindle-polarity coupling and centrosome organization. *Nat. Cell Biol.* 8:586–593. doi:10.1038/ncb1409

Jaffe, A.B., N. Kaji, J. Durgan, and A. Hall. 2008. Cdc42 controls spindle orientation to position the apical surface during epithelial morphogenesis. *J. Cell Biol.* 183:625–633. doi:10.1083/jcb.200807121

Johnston, C.A., K. Hirono, K.E. Prehoda, and C.Q. Doe. 2009. Identification of an Aurora-A/PinsLINKER/Dlg spindle orientation pathway using induced cell polarity in S2 cells. *Cell.* 138:1150–1163. doi:10.1016/j.cell.2009.07.041

Kaushik, R., F. Yu, W. Chia, X. Yang, and S. Bahri. 2003. Subcellular localization of LGN during mitosis: evidence for its cortical localization in mitotic cell culture systems and its requirement for normal cell cycle progression. *Mol. Biol. Cell.* 14:3144–3155. doi:10.1091/mbc.E03-04-0212

Kisurina-Evgenieva, O., G. Mack, Q. Du, I. Macara, A. Khodjakov, and D.A. Compton. 2004. Multiple mechanisms regulate NuMA dynamics at spindle poles. *J. Cell Sci.* 117:6391–6400. doi:10.1242/jcs.01568

Konno, D., G. Shioi, A. Shitamukai, A. Mori, H. Kiyonari, T. Miyata, and F. Matsuzaki. 2008. Neuroepithelial progenitors undergo LGN-dependent planar divisions to maintain self-renewability during mammalian neurogenesis. *Nat. Cell Biol.* 10:93–101. doi:10.1038/ncb1673

Martin-Belmonte, F., A. Gassama, A. Datta, W. Yu, U. Rescher, V. Gerke, and K. Mostov. 2007. PTEN-mediated apical segregation of phosphoinositides controls epithelial morphogenesis through Cdc42. *Cell.* 128:383–397. doi:10.1016/j.cell.2006.11.051

Mayer, T.U., T.M. Kapoor, S.J. Haggarty, R.W. King, S.L. Schreiber, and T.J. Mitchison. 1999. Small molecule inhibitor of mitotic spindle bipolarity identified in a phenotype-based screen. *Science.* 286:971–974. doi:10.1126/science.286.5441.971

McCudden, C.R., F.S. Willard, R.J. Kimple, C.A. Johnston, M.D. Hains, M.B. Jones, and D.P. Siderovski. 2005. G alpha selectivity and inhibitor function of the multiple GoLoco motif protein GPSM2/LGN. *Biochim. Biophys. Acta.* 1745:254–264. doi:10.1016/j.bbamcr.2005.05.002

Merdes, A., K. Ramyar, J.D. Vechio, and D.W. Cleveland. 1996. A complex of NuMA and cytoplasmic dynein is essential for mitotic spindle assembly. *Cell.* 87:447–458. doi:10.1016/S0092-8674(00)81365-3

Mitsushima, M., F. Toyoshima, and E. Nishida. 2009. Dual role of Cdc42 in spindle orientation control of adherent cells. *Mol. Cell. Biol.* 29:2816–2827. doi:10.1128/MCB.01713-08

Morin, X., F. Jaouen, and P. Durbec. 2007. Control of planar divisions by the G-protein regulator LGN maintains progenitors in the chick neuroepithelium. *Nat. Neurosci.* 10:1440–1448. doi:10.1038/nn1984

Nipper, R.W., K.H. Siller, N.R. Smith, C.Q. Doe, and K.E. Prehoda. 2007. Galphai generates multiple Pins activation states to link cortical polarity and spindle orientation in *Drosophila* neuroblasts. *Proc. Natl. Acad. Sci. USA.* 104:14306–14311. doi:10.1073/pnas.0701812104

O'Brien, L.E., M.M. Zegers, and K.E. Mostov. 2002. Opinion: Building epithelial architecture: insights from three-dimensional culture models. *Nat. Rev. Mol. Cell Biol.* 3:531–537. doi:10.1038/nrm859

Park, D.H., and L.S. Rose. 2008. Dynamic localization of LIN-5 and GPR-1/2 to cortical force generation domains during spindle positioning. *Dev. Biol.* 315:42–54. doi:10.1016/j.ydbio.2007.11.037

Rappaport, R. 1971. Cytokinesis in animal cells. *Int. Rev. Cytol.* 31:169–213. doi:10.1016/S0074-7696(08)60059-5

Roegiers, F., and Y.N. Jan. 2004. Asymmetric cell division. *Curr. Opin. Cell Biol.* 16:195–205. doi:10.1016/j.ceb.2004.02.010

Roh, M.H., O. Makarova, C.J. Liu, K. Shin, S. Lee, S. Laurinec, M. Goyal, R. Wiggins, and B. Margolis. 2002. The Maguk protein, Pals1, functions as an adapter, linking mammalian homologues of Crumbs and Discs Lost. *J. Cell Biol.* 157:161–172. doi:10.1083/jcb.200109010

Roh, M.H., S. Fan, C.J. Liu, and B. Margolis. 2003. The Crumbs3-Pals1 complex participates in the establishment of polarity in mammalian epithelial cells. *J. Cell Sci.* 116:2895–2906. doi:10.1242/jcs.00500

Saburi, S., I. Hester, E. Fischer, M. Pontoglio, V. Eremina, M. Gessler, S.E. Quaggin, R. Harrison, R. Mount, and H. McNeill. 2008. Loss of Fat4 disrupts PCP signaling and oriented cell division and leads to cystic kidney disease. *Nat. Genet.* 40:1010–1015. doi:10.1038/ng.179

Sanada, K., and L.H. Tsai. 2005. G protein betagamma subunits and AGS3 control spindle orientation and asymmetric cell fate of cerebral cortical progenitors. *Cell.* 122:119–131. doi:10.1016/j.cell.2005.05.009

Sans, N., P.Y. Wang, Q. Du, R.S. Petralia, Y.X. Wang, S. Nakka, J.B. Blumer, I.G. Macara, and R.J. Wenthold. 2005. mPins modulates PSD-95 and SAP102 trafficking and influences NMDA receptor surface expression. *Nat. Cell Biol.* 7:1179–1190. doi:10.1038/ncb1325

Segalen, M., and Y. Bellaïche. 2009. Cell division orientation and planar cell polarity pathways. *Semin. Cell Dev. Biol.* 20:972–977. doi:10.1016/j.semcdb.2009.03.018

Siegrist, S.E., and C.Q. Doe. 2005. Microtubule-induced Pins/Galphai cortical polarity in *Drosophila* neuroblasts. *Cell.* 123:1323–1335. doi:10.1016/j.cell.2005.09.043

Siegrist, S.E., and C.Q. Doe. 2006. Extrinsic cues orient the cell division axis in *Drosophila* embryonic neuroblasts. *Development.* 133:529–536. doi:10.1242/dev.02211

Siller, K.H., and C.Q. Doe. 2009. Spindle orientation during asymmetric cell division. *Nat. Cell Biol.* 11:365–374. doi:10.1038/ncb0409-365

Siller, K.H., C. Cabernard, and C.Q. Doe. 2006. The NuMA-related Mud protein binds Pins and regulates spindle orientation in *Drosophila* neuroblasts. *Nat. Cell Biol.* 8:594–600. doi:10.1038/ncb1412

Tall, G.G., and A.G. Gilman. 2005. Resistance to inhibitors of cholinesterase 8A catalyzes release of Galphai-GTP and nuclear mitotic apparatus protein (NuMA) from NuMA/LGN/Galphai-GDP complexes. *Proc. Natl. Acad. Sci. USA.* 102:16584–16589. doi:10.1073/pnas.0508306102

Théry, M., and M. Bornens. 2006. Cell shape and cell division. *Curr. Opin. Cell Biol.* 18:648–657. doi:10.1016/j.ceb.2006.10.001

Théry, M., A. Jiménez-Dalmaroni, V. Racine, M. Bornens, and F. Jülicher. 2007. Experimental and theoretical study of mitotic spindle orientation. *Nature.* 447:493–496. doi:10.1038/nature05786

Toyoshima, F., and E. Nishida. 2007. Integrin-mediated adhesion orients the spindle parallel to the substratum in an EB1- and myosin X-dependent manner. *EMBO J.* 26:1487–1498. doi:10.1038/sj.emboj.7601599

Toyoshima, F., S. Matsumura, H. Morimoto, M. Mitsushima, and E. Nishida. 2007. PtdIns(3,4,5)P3 regulates spindle orientation in adherent cells. *Dev. Cell.* 13:796–811. doi:10.1016/j.devcel.2007.10.014

Willard, F.S., R.J. Kimple, and D.P. Siderovski. 2004. Return of the GDI: the GoLoco motif in cell division. *Annu. Rev. Biochem.* 73:925–951. doi:10.1146/annurev.biochem.73.011303.073756

Willard, F.S., Z. Zheng, J. Guo, G.J. Digby, A.J. Kimple, J.M. Conley, C.A. Johnston, D. Bosch, M.D. Willard, V.J. Watts, et al. 2008. A point mutation to Galphai selectively blocks GoLoco motif binding: direct evidence for Galpha.GoLoco complexes in mitotic spindle dynamics. *J. Biol. Chem.* 283:36698–36710. doi:10.1074/jbc.M804936200

Yasumi, M., T. Sakisaka, T. Hoshino, T. Kimura, Y. Sakamoto, T. Yamanaka, S. Ohno, and Y. Takai. 2005. Direct binding of Lgl2 to LGN during mitosis and its requirement for normal cell division. *J. Biol. Chem.* 280:6761–6765. doi:10.1074/jbc.C400440200

Yu, W., L.E. O'Brien, F. Wang, H. Bourne, K.E. Mostov, and M.M. Zegers. 2003. Hepatocyte growth factor switches orientation of polarity and mode of movement during morphogenesis of multicellular epithelial structures. *Mol. Biol. Cell.* 14:748–763. doi:10.1091/mbc.E02-06-0350